ISBN: 978-3-95450-247-9 ISSN: 2673-5490 doi: 10.18429/JACoW-IPAC2024-THPC13

OPTICS DESIGN OF A COMPACT HELIUM SYNCHROTRON FOR ADVANCED CANCER THERAPY

H. Huttunen*[1], F. Asvesta, D. Flier[2], L. Bottura, T. Prebibaj,
R. Taylor, M. Vretenar, CERN, Geneva, Switzerland
E. Benedetto, SEEIIST, Geneva, Switzerland & Tera-Care, Geneva, Switzerland
[1] also at University of Helsinki, Helsinki, Finland
[2] also at University of Twente, Enschede, Netherlands

Abstract

The design of a helium synchrotron for cancer therapy is being studied and optimized in the context of the Next Ion Medical Machine Study (NIMMS) at CERN. In particular, the effects of combined-function magnets and their geometry on the optics functions and hence on the beam size are evaluated. Moreover, the introduction of defocusing quadrupoles in the lattice is investigated as a means of better controlling the optics in both planes, while sextupoles for chromaticity control and resonant extraction are introduced. The updated lattice design is simulated to identify potential limitations in terms of nonlinear dynamics due to the low periodicity of the lattice and propose a regime for operations from the transverse beam dynamics' perspective.

INTRODUCTION

The Next Ion Medical Machine Study (NIMMS) is a CERN-based collaboration that develops next generation ion therapy facilities for advanced cancer treatment [1]. The current baseline for the conceptual design of the Helium Light Ion Compact Synchrotron (HeLICS) is a triangular layout optimized for acceleration of protons and alpha particles (He_4^{2+} ions) [2]. The optics of HeLICS aims for compactness and simplicity with a circumference of 33 m.

The lattice consists of three bending units connected by straight sections of zero dispersion. The bending units consists of two 60° combined function main magnets and a quadrupole between them. They provide the means for beam bending and dispersion control within the straight sections. The straight sections are designed to accommodate injection septa, extraction septa and the RF cavity. Each straight section also contains two focusing quadrupoles to control the horizontal tune. In the absence of dedicated defocusing quadrupoles, all defocusing in the lattice is provided by the combined function main magnets. The helium beam is accelerated from 5 MeV/u up to 220 MeV/u to achieve a penetration depth of 30 cm in water, sufficient to cover the maximum depth of tumors under consideration [2, 3]. Multi-turn injection is utilized to achieve high enough beam intensity [2]. In addition, a horizontal tune near the 3rd integer resonance is required for slow extraction [4].

An initial optics configuration for HeLICS has been defined for a flat-top working point near the 3rd order resonance at $Q_x = 2.67$, $Q_y = 0.7$. This working point results in maximum beta functions of $\beta_{x,max} \approx 26$ m and $\beta_{y,max} \approx 15$ m, both too high for the aperture requirements. Due to the absence of defocusing quadrupoles, the vertical tune cannot be changed independently but varies along with the horizontal tune as the focusing quadrupole strength is changed. This limited flexibility could lead to issues in operation due to nonlinear resonances that might not be avoided. In addition, the high quadrupolar gradient of the combined function magnets can have a negative effect to the good field region limiting the aperture even further. To address these challenges, several lattice optimisations have been explored.

LINEAR OPTICS OPTIMIZATION

The compactness of the HeLICS lattice leads to strict constraints in optics design. Aperture requirements of the dipoles limit the vertical beta function to $\beta_{y,\max}$<10 m, which corresponds to a $\pm 3\sigma$ beam size of $\pm$30 mm. In turn, the horizontal beta function should be maintained at $\beta_{x,\max}$<20 m to keep the horizontal $\pm 3\sigma$ beam size below $\pm$75 mm in the straight section. Assumed emittances and other relevant beam parameters are presented in Table 1.

Table 1: Expected Helium Beam Parameters at Injection

Bunch population I	8.2e10
Horizontal normalized emittance $\epsilon_{n,x}$	3 mm mrad
Vertical normalized emittance $\epsilon_{n,y}$	1 mm mrad
Maximum momentum spread $(\Delta p/p)_{\max}$	1e-3
Relativistic factor β_{rel}	0.103

Dipole Modeling

The initial requirements for the combined function magnets consist of a 60° bending angle, a vertical aperture of 70 mm, and a central magnetic field strength of 1.65 T with a gradient of 1.1 T/m. Existing synchrotrons such as CLS, ALBA, SESAME and PS employ combined function main magnets [5–8]. However, these magnets feature lower bending angles, lower central magnetic field strengths and, with the exception of the PS, much smaller vertical apertures, compared to the proposed design. Meeting the specified requirement for the field uniformity of $\frac{\Delta B}{B} \leq$ 5e-4 while maintaining a compact design was challenging. Therefore reducing the combined-function gradient with edge focusing was proposed, which facilitates a reduction in aperture width [9]. As a result, the coil operates at a modest current

* heli.huttunen@cern.ch

ISBN: 978-3-95450-247-9 ISSN: 2673-5490 doi: 10.18429/JACoW-IPAC2024-THPC13

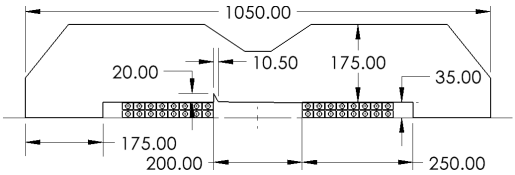

Figure 1: Half cross-section of the compact dipole magnet.

density of 10 A/mm^2, which is compatible with water cooling. The required massflow is such that the water velocity is below 3 m/s, to avoid erosion issues.

The 2D magnet design of the proposed solution with a gradient of 0.5 T/m is depicted in Fig. 1, which optimizes both compactness and field homogeneity within ±5e-4. At injection, the magnetic efficiency is 99.7% but drops to 92.3% during extraction due to iron saturation effects.

Updated Lattice Design

The optics optimization of a compact accelerator with a limited number of elements is challenging. For HeLICS, possible optimization methods were limited to changing the geometry of the main magnets, finding a more optimal operating tune or introducing new corrector elements such as weak defocusing quadrupoles.

First, the impact of the horizontal working point on the optics functions was investigated. Working points near the third integer resonances at $Q_x = 2.67$ or 2.33 were considered. At $Q_x = 2.33$ the $\beta_{x,\max}$ decreased significantly while $\beta_{y,\max}$ remained the same. Consequently, this working point is considered as the new baseline.

A sector magnet, such as the ones used in the HeLICS initial optics, does not provide any vertical edge focusing [10]. To this end, the possibility of adding focusing to the lattice through the pole face angles of the bending edges was explored, as commonly used in compact synchrotrons [11]. The aim was to examine the impact of this effect both on the magnitude of $\beta_{y,\max}$ and the combined function gradient. A configuration shown in Fig. 2 was proposed, where a 30° angle is introduced to both entrance and exit of the magnets, effectively turning the sector bend into a rectangular bend. With this modification, $\beta_{y,\max}$ could be reduced to about 9 m, which complies with the aperture requirements. At the same time, the combined function gradient was reduced from 1.1 T/m to 0.7 T/m, not quite enough to meet the 0.5 T/m design requirement.

The lattice was further developed to include defocusing quadrupole magnets. In this manner, a larger tune space

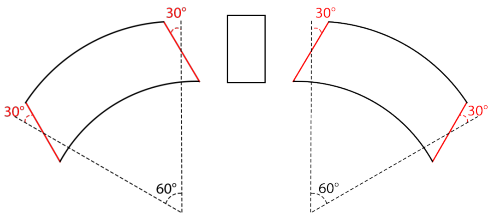

Figure 2: HeLICS bending unit with 30° edges.

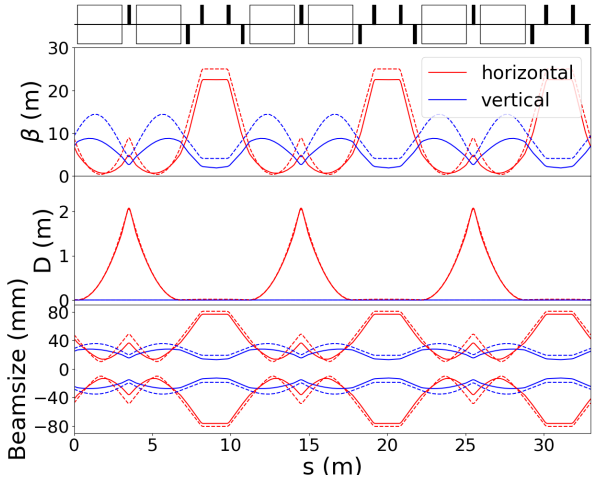

Figure 3: Initial (dashed) and updated (solid) HeLICS optics, from top to bottom: lattice (main magnets shown as white rectangeles, focusing quadrupoles shown as black upward rectangles and defocusing quadrupoles shown as black downward rectangles), beta functions, dispersion, 3 sigma beamsize estimated for the parameters of Table 1.

becomes accessible also in the vertical plane, at the price of introducing an extra quadrupole family. Finally, with these modifications the β-functions were reduced to 22 m and 9 m in x and y respectively. Figure 3 shows the updated optics functions after the implementation of these changes.

CHROMATICITY SEXTUPOLES

According to the Hardt condition, the separatrices of different momenta can be aligned to the electrostatic extraction septum [12]. In the zero dispersion region, the Hardt condition is satisfied when the chromaticity is set to zero. The natural chromaticities of the updated HeLICS lattice are $Q'_x = -3.4$ and $Q'_y = -3.1$ near the extraction working point. To minimize losses on the electrostatic septum, chromaticity correction in the horizontal plane is thus necessary [13]. Clinical requirements for dose homogeneity also impose a need for low chromaticity in RF Knock Out extraction [14].

Sextupoles for chromaticity correction need to be installed in a non-zero dispersion region [15]. In the case of the HeLICS lattice, this is problematic because the dispersion in the straight section is set to zero, while the bending unit is designed to be so compact that it cannot readily accommodate any extra elements. As a result two options were considered.

As a first option, the dispersion in the straight section was increased to 0.5 m. In this case, correcting the horizontal chromaticity to zero would require strong sextupoles. The benefit of adding sextupoles to the straight section is the possibility of integrating them into the defocusing quadrupoles to maintain compactness. However, in the case of strong sextupoles this advantage would be lost.

It was therefore decided to explore the possibility of placing the sextupoles in the bending unit instead. The short

ISBN: 978-3-95450-247-9 ISSN: 2673-5490 doi: 10.18429/JACoW-IPAC2024-THPC13

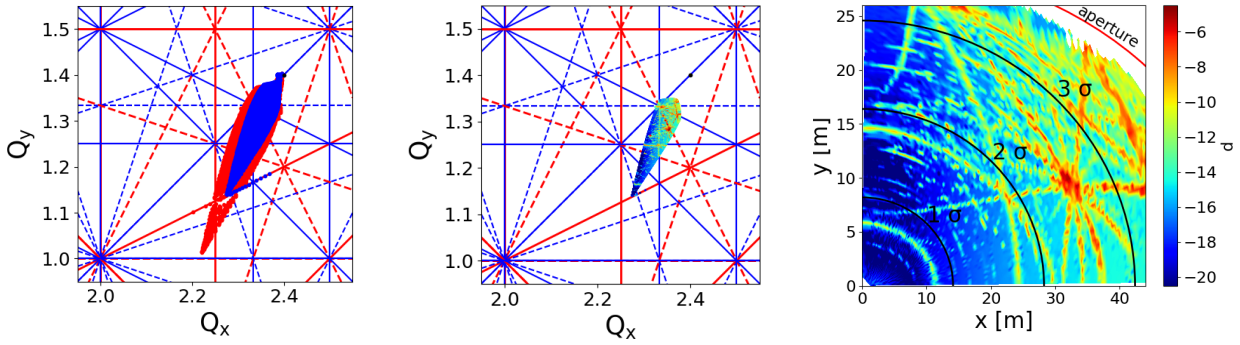

Figure 4: Tune spread reduction between a Gaussian (red) and a more parabolic (blue) longitudinal profile (left), FMA showing the the tune footprint (middle) and the initial particle coordinates (right) color coded with the tune diffusion.

straight section in the bending unit was made 0.7 m longer to accommodate the sextupoles. This increased the total circumference of the lattice to 35 m. Changing the length of the lattice also affected the optics and further reduced the β functions to about 18 and 8 m in the horizontal and vertical planes respectively. This is equivalent to a reduction of more than 45% and 20% in the two planes accordingly, and finally brought both β functions below the desired limits. Simultaneously, the gradient of the combined function is reduced to 0.5 T/m, which is the desired value from a dipole design point of view. The sextupoles were placed in the bending unit after the quadrupole. Assuming a sextupole length of 0.2 m, the maximum required strength for the sextupoles to set the horizontal chromaticity to zero is 35 T/m^2. When the chromaticity in the horizontal plane was set to zero, the vertical one increased to $Q'_y = -6.0$.

TRACKING SIMULATIONS

The HeLICS lattice has a periodicity of only 3, which can lead to reduced stability as many systematic resonances are present [16]. To analyze weakly chaotic motion in Hamiltonian systems, the Frequency Map Analysis (FMA) technique [17,18] can be applied to tracking data including space charge effects to study the excitation of space charge driven resonances [19]. The Numerical Analysis of Fundamental Frequencies (NAFF) is applied to the turn-by-turn data to calculate the tunes of individual particles [20,21].

Initially, the space charge induced tune spread was estimated analytically [22] assuming a bunching factor of 0.7. Such a high bunching factor resulted in a small tune shift $\Delta Q_x = -0.06$ and $\Delta Q_y = -0.10$. However, a Gaussian longitudinal profile with an RMS bunch length of 3 m results in tune shifts of $\Delta Q_x = -0.18$ and $\Delta Q_y = -0.36$, as shown in Fig. 4 with red. Assuming a more parabolic longitudinal profile, the decreased line density will result in slightly lower tune spread, as shown in Fig. 4 with blue. Nevertheless, the tune spread remains much higher than what was assumed initially. To further reduce the tune spread, additional RF systems for double or triple harmonic operation should be investigated [23].

Figure 4 shows the FMA of the HeLICS lattice for the more parabolic longitudinal profile for on-momentum particles with space charge. The tune diffusion rate is estimated from the tune variation along the particle trajectory [17] as $d = \log\sqrt{(Q_{x,2} - Q_{x,1})^2 + (Q_{y,2} - Q_{y,1})^2}$, with the subscripts 1 and 2 referring to the first and second synchrotron period, respectively. The aperture of the machine is included in the simulations, and particles close to the aperture did not survive. The diffusion increases above 2σ beam size at the injection working point $Q_x = 2.4$, and some excited resonances are observed. It is necessary to explore other working points to avoid this region of higher diffusion.

CONCLUSION

The HeLICS optics were adjusted to reduce the gap of the main dipoles, and lower the combined function gradient to 0.5 T/m, profiting from edge focusing. This increases the magnetic efficiency, as well as lowers the operating current and cooling requirements. The main dipole coils operate at a current density of 10 A/mm^2, which is compatible with water cooling at speed below erosion limits. The horizontal working point for extraction is switched from 2.67 to 2.33 to reduce $\beta_{x,\max}$. A pole face angle of 30° is added to the bending magnets to gain vertical focusing, effectively turning the original sector magnets into rectangular magnets. In addition, defocusing quadrupoles are added to the lattice for flexibility. A 0.7 m space is inserted in between the bending units to accommodate for chromaticity sextupoles. With the implemented changes, horizontal and vertical β functions are reduced by more than 20% and 45% respectively. The combined function gradient of the dipoles is also reduced by half to meet the design requirements. The first tracking simulations are carried out with the optimized lattice. It is found that the space charge induced tune spread of a single harmonic Gaussian profile is too large, and other solutions need to be explored. Furthermore, some driven resonances and high diffusion beyond 2σ beam size are observed from the FMA at the injection tune $Q_x = 2.4$. This requires further investigation, and other working points must be considered.

ACKNOWLEDGEMENTS

The authors would like to express special thanks to Dr Simon Albright and Dr Giovanni Iadarola for their help.

ISBN: 978-3-95450-247-9 ISSN: 2673-5490 doi: 10.18429/JACoW-IPAC2024-THPC13

REFERENCES

[1] M. Vretenar *et al.*, "The next ion medical machine study at CERN: Towards a next generation cancer research and therapy facility with ion beams", in *Proc. IPAC'21*, Campinas, Brazil, May 2021, pp. 1240-1243. doi:10.18429/JACoW-IPAC2021-MOPAB413

[2] E. Benedetto and M. Vretenar, "Innovations in the next generation medical accelerators for therapy with ion beams", *J. Phys.: Conf. Ser.*, vol. 2687, pp. 5083-5086 , Jan. 2024. doi:10.1088/1742-6596/2687/9/092003

[3] M. Vretenar *et al.*, "A compact synchrotron for advanced cancer therapy with helium and proton beams", *J. Phys.: Conf. Ser.*, vol. 2420, pp. 811–814, Jan. 2023. doi:10.1088/1742-6596/2420/1/012103

[4] R. Taylor, E. Benedetto, M. Sapinski, and J. Pasternak, "Slow extraction modelling for NIMMS hadron therapy synchrotrons", *J. Phys.: Conf. Ser.*, vol. 2420, pp. 2988-2991, Jan. 2023. doi:10.1088/1742-6596/2420/1/012101

[5] L. Dallin *et al.*, "Gradient dipole magnets for the Canadian light source", in *Proc. EPAC'02*, Paris, France, Jun. 2002, pp. 2340-2342. cds.cern.ch/record/584810

[6] M. Pont, E. Boter, and M. Lopes, "Magnets for the storage ring ALBA", in *Proc. EPAC'06*, Edinburgh, UK, Jun. 2006, pp. 2562-2564.

[7] A. Milanese, E. Huttel, and M. M. Shehab, "Design of the main magnets of the SESAME storage ring", in *Proc. IPAC'14*, Dresden, Germany, Jun. 2014, pp. 1292–1294. doi:10.18429/JACoW-IPAC2014-TUPRO105

[8] M. Juchno, "Magnetic model of the CERN proton synchrotron main magnetic unit", 2011. cds.cern.ch/record/1407908

[9] J. Tanabe, "Iron dominated electromagnets: design, fabrication, assembly and measurements", Technical Report, SLAC-R-754, United States, Sep. 2005. doi:10.2172/878409

[10] V. Kumar and A. Sharma, "Understanding the edge focusing in dipole magnets", in *Indian Particle Accelerator Conference 2018*, Jan. 2018, pp. 776-778.

[11] M. Umezawa *et al.*, "Development of compact proton beam therapy system for moving organs", *Hitachi Review*, vol. 64, no. 8, p. 506. 2015. api.semanticscholar.org/CorpusID:21954106

[12] M. Pullia, "Hardt condition for superposition of separatrices", 1996.

[13] L. Badano *et al.*, "Proton-Ion Medical Machine Study (PIMMS), 1", 2000. cds.cern.ch/record/385378

[14] S. Savazzi *et al.*, "Implementation of RF-KO extraction at CNAO", *Proc. IPAC'19*, Melbourne, Australia, May 2019, pp. 3469-3471. doi:10.18429/JACoW-IPAC2019-THPMP010

[15] S. Lee, "Accelerator physics", 1999.

[16] H. Wiedemann, "Particle Accelerator Physics", 2015, pp. 539-564.

[17] J. Laskar, "Frequency analysis for multi-dimensional systems. Global dynamics and diffusion", *Physica D: Nonlinear Phenomena*, vol. 67, pp. 257-281, 1993. doi:10.1016/0167-2789(93)90210-R

[18] Y. Papaphilippou, "Detecting chaos in particle accelerators through the frequency map analysis method", *Chaos*, vol. 24, 2014. doi:10.1063/1.4884495

[19] F. Asvesta *et al.*, "Identification and characterization of high order incoherent space charge driven structure resonances in the CERN Proton Synchrotron", *Phys. Rev. Accel. Beams*, vol. 23, 2020. doi:10.1103/PhysRevAccelBeams.23.091001

[20] J. Laskar, C. Froeschlé, and A. Celletti, "The measure of chaos by the numerical analysis of the fundamental frequencies. Application to the standard mapping", *Physica D: Nonlinear Phenomena*, vol. 56, Amsterdam, 1992. doi:10.1016/0167-2789(92)90028-L

[21] F. Asvesta, N. Karastathis, and P. Zisopoulos, "Computer code PyNAFF". github.com/nkarast/PyNAFF

[22] K. Schindl, "Space Charge", CERN, Geneva, Switzerland, CERN/PS 99-012(DI), 1999.

[23] F. Asvesta *et al.*, "Pushing high intensity and high brightness limits in the CERN PSB after the LIU upgrades", in *Proc. HB'23*, Geneva, Switzerland, Oct. 2023, p. 458. doi:10.18429/JACoW-HB2023-THBP09